A Fast Crosshole Electromagnetic Tomography Using Localized Nonlinear Approximation

Hee Joon Kim[1], Ki Ha Lee[2], and Mike Wilt[3]

1. Introduction

High-resolution imaging of electrical conductivity has been the subject of many studies in crosshole tomography using electromagnetic (EM) fields (Zhou et al., 1993; Wilt et al., 1995; Alumbaugh and Morrison, 1995; Newman, 1995; Alumbaugh and Newman, 1997). Although the theoretical understanding and associated field practices for crosshole EM methods are relatively mature, fast and stable imaging of crosshole EM data is still a challenging problem.

The main advantage of integral equation (IE) method over the finite difference (FD) and/or finite-element (FE) methods is its greater suitability for inversion. For example, IE formulation readily contains a sensitivity matrix, which can be revised at each inversion iteration at little expense. With the FD or FE method, in contrast, the sensitivity matrix has to be recomputed at each iteration at a cost nearly equal to that of full forward modeling. The IE method, however, has to overcome severe practical limitations imposed on the size of imaging domain for inversion purposes. In this direction, several approximate methods such as localized nonlinear (LN) approximation (Habashy et al., 1993) and quasi-linear approximation (Zhdanov and Fang, 1996) have been developed. Recently, Lee et al. (2002) applied the LN approximation for a cylindrically symmetric model to inverting single-hole EM data.

In this paper an advantage of the LN approximation is exploited with applications to crosshole EM tomography. We begin our discussion with a critical check of the accuracy of LN approximation for a cylindrically symmetric model. We then describe our EM tomography algorithm and demonstrate the stability and effectiveness of this approach by inverting synthetic data. Finally, we present an example application to field data measured as a part of the Lost Hills CO_2 pilot project in southern California, U. S. A.

2. LN approximation

The LN approximation of IE solutions for a cylindrically symmetric model is described in detail in Lee et al. (2002). For completeness, their work is briefly outlined here.

To illustrate the efficiency and usefulness of the LN numerical solution in a crosshole application, let us consider a simple model consisting of a conductive ring about a source borehole axis in a uniform whole space of 100 ohm-m. The cross-section of the ring is a 10 m by 10 m rectangle and 15 m horizontally away from the borehole as shown in Figure 1. The Born and LN approximated magnetic fields measured in the other borehole 50 m horizontally away from the source borehole are compared with results obtained from a full FE method (Lee et al., 2003).

Figure 2 shows the comparison in secondary horizontal and vertical magnetic fields between Born, LN, and FE solutions. The center of the body is chosen as $z = 0$. The conductivity contrast and operating frequency used are 10 and 10 kHz, respectively. The source and receiver are located at the same depth in each borehole. More anomalies can be observed in the imaginary part than in the real part. For all field components, the LN and FE solutions agree very well.

We are also interested in the quality of LN solutions when the conductivity of the body is varied. Figure 3 shows the comparison in secondary vertical magnetic fields between Born, LN, and FE solutions. A vertical magnetic dipole source is fixed at the depth of the center of body in the source borehole, and vertical magnetic fields are measured at 10 m below the center of the body in the receiver borehole. The frequency used is 10 kHz. The LN approximation is very well up to the conductivity contrast of about 100. The imaginary part of the LN solution starts deviating from the FE solution beyond the conductivity contrast of 100, while the real part still shows a good agreement.

Finally, the comparison is made for responses in frequency as shown in Figure 4. The source-receiver array is the same as that in Figure 3, and the conductivity contrast is fixed to 10. The LN and FE

Key words: crosshole, tomography, electromagnetic, localized nonlinear approximation

1) Pukyong National University, Korea (hejkim@pknu.ac.kr)

2) Lawrence Berkeley National Laboratory (KHLee@lbl.gov)

3) ElectroMagnetic Instruments, Inc. (wilt@emiinc.com)

solutions show a good agreement all the way up to about 100 kHz.

3. Inversion

Based on the encouraging results of the LN approximation, we have proceeded to implement crosshole EM tomography. Measurements are made in the other borehole to the source borehole

To evaluate the performance of the crosshole tomography using the LN approximation, we choose a conductivity model shown in Figure 5. The model consists of two cylindrically symmetric bodies, one conductive (0.1 S/m) and the other resistive (0.001 S/m), in a whole space of 0.01 S/m. A FE scheme (Lee et al., 2002) is used to generate synthetic data. Using a vertical magnetic dipole (M_z) as a source, vertical magnetic fields (H_z) are computed at three frequencies of 2.5 kHz, 10 kHz and 20 kHz. Three-percent Gaussian noise is added to the synthetic data prior to the inversion. The inversion is started with an initial model of 60 ohm-m uniform whole space.

After 8 iterations, the two bodies are clearly reconstructed as shown in Figure 6. The recovered conductivity is found to be nearly the same in the conductive body but is overestimated in the resistive body. The inversion process is quite stable, and the rms misfit decreases from the initial guess of 5.095 to 0.036 after 8 iterations. The smoothing parameter varies significantly during the inversion process. This means it is difficult to determine the parameter a priori.

Finally, our tomography algorithm has been applied to a set of crosshole field data provided by Chevron as a part of the Lost Hills CO_2 pilot project in southern California (Wilt, 2002). The separation between the two vertical boreholes is 24.536 m and CO_2 injection well is near the center of the section defined by the two wells. Although both EM and seismic data for the pre- and post-injection of CO_2 are available, we conducted tomographic inversion using only EM (M_z-H_z) data. The operating frequency was 759 Hz.

Figure 7 shows inversion results of the crosshole data. The CO_2 injection into a reservoir of oil/brine mixture results in changes in conductivity, which can be indirectly interpreted as the displacement of brine with injected CO_2. The replacement of water with CO_2 makes a decrease of conductivity. Figure 7 shows a significant change in resistivity distribution, and this increase of resistivity suggests an effect of the CO_2 injection. Unfortunately, the borehole separation is not far enough compared with the skin depth (i.e., low frequency), the reconstructed images using the assumption of cylindrically symmetry may have artifacts that can be produced by the geometry of conductive zone outside of the interwell plane (Alumbaugh and Morrison, 1995). Computing time required for this approximate tomography is less than 5 minutes on a Pentium-4 PC to obtain 650 conductivities from 604 complex H_z fields after 5 iterations.

4. Conclusions

The LN approximation of IE solutions has been applied to inverting crosshole EM data using a cylindrically symmetric model. The LN approximation is less accurate than an exact solution but much superior to the simple Born approximation. Moreover, when applied to the cylindrically symmetric model with a vertical magnetic dipole source, the accuracy of LN approximation is greatly improved because electric fields are scalar and continuous everywhere. One of the most important steps in the inversion is the selection of a proper regularization parameter for stability. The LN solution provides an efficient means for selecting an optimum regularization parameter, because Green's functions, the most time consuming part in IE methods, are repeatedly re-usable at each iteration. In addition, the IE formulation readily contains a sensitivity matrix, which can be revised at each iteration at little expense. This fast imaging scheme has been tested on its stability and efficiency using synthetic and field data. The reconstructed image from the field data is comparable with other geophysical data.

Acknowledgements

Korea Science and Engineering Foundation (R01-2001-000071-0) provided support for this study. This work was also supported by the Assistant Secretary for Energy Efficiency and Renewable Energy, Office of Wind and Geothermal Technologies of the U.S. Department of Energy under Contract No. DE-AC03-76SF00098. We would like to thank Michael Morea, Chevron USA Production Company, and the US Department of Energy, National Petroleum Technology Office, (Class III Field Demonstration Project DE-FC22-95BC14938) for allowing us to publish this data.

References

Alumbaugh, D. L. and Morrison, H.F., 1995, Theoretical and practical considerations for crosswell electromagnetic tomography assuming a cylindrical geometry, *Geophysics*, **60**, 846-870.

Alumbaugh, D. L., and Newman, G. A., 1997, Three-dimensional massively parallel electromagnetic inversion—II. Analysis of crosswell electromagnetic experiment, *Geophys. J. Int.*, **128**, 355-363.

Habashy, T. M., Groom, R. M., and Spies, B. R., 1993, Beyond the Born and Rytov approximations: a nonlinear approach to electromagnetic scattering, *J. Geophys. Res.*, **98**, 1795-1775.

Lee, K. H., Kim, H. J., and Uchida, T., 2003, Electromagnetic fields in steel-cased borehole, *Geophys. Prosp.* (submitted)

Lee, K. H., Kim, H. J., and Wilt, M., 2002, Efficient imaging of single-hole electromagnetic data, *Geothermal Resources Council Transactions*, **26**, 399-404.

Newman, G. A., 1995, Crosswell electromagnetic inversion using integral and differential equations, *Geophysics*, **60**, 899-911.

Wilt, M. J., Alumbaugh, D. L., Morrison, H. F., Becker, A., Lee, K. H., and Deszcz-Pan, M., 1995, Crosshole electromagnetic tomography: System design considerations and field results: *Geophysics*, **60**, 871-885.

Wilt, M. J., Mallan, R., Kasameyer, P., and Kirkendall, B., 2002, Extended 3D induction logging for geothermal resource assessment: Field results with the Geo-BILT system, Proc. 27th Workshop on Geothermal Reservoir Engineering, Stanford Univ., SGP-TR-171.

Zhou, Q., Becker, A., and Morrison, H. F., 1993, Audio-frequency electromagnetic tomography in 2-D, *Geophysics*, **58**, 482-495.

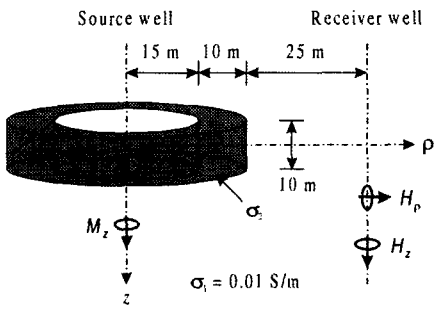

Fig. 1.

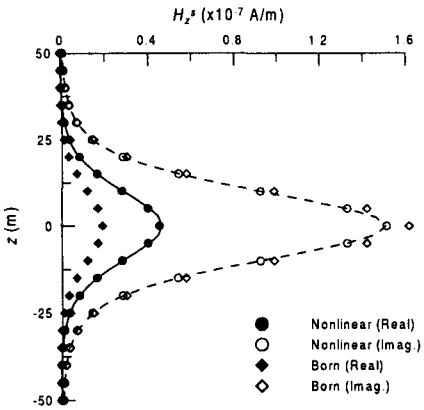

Fig. 2.

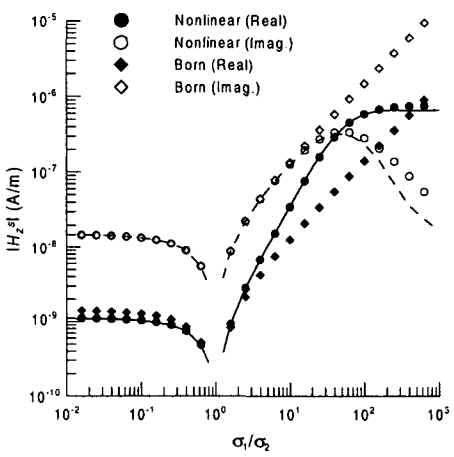

Fig. 3.

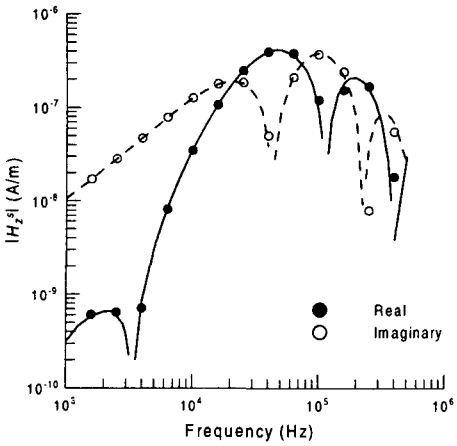

Fig. 4.

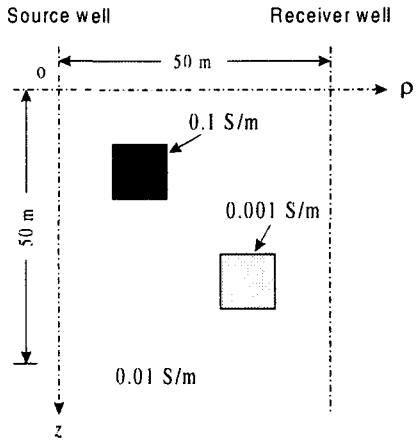

Fig. 5.

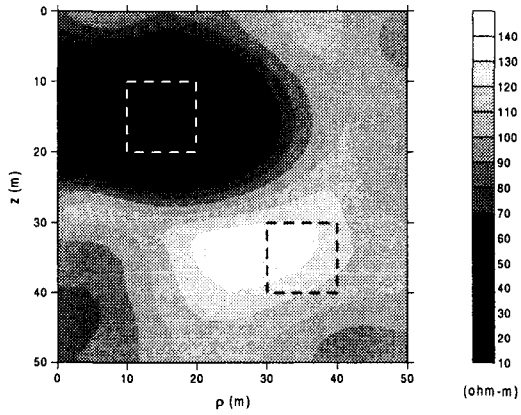

Fig. 6.

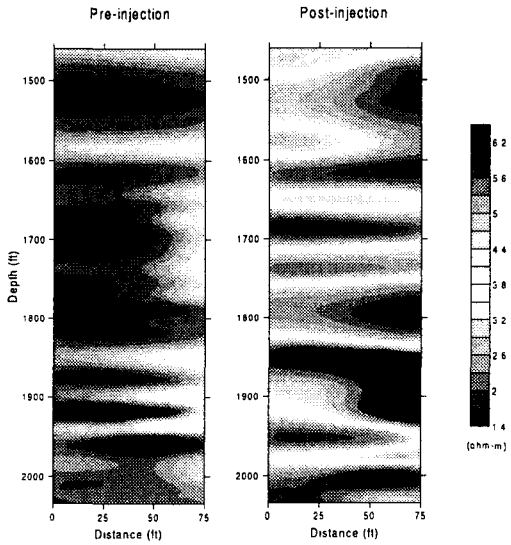

Fig. 7.